

Mass Transfer of CO₂ into Water and Surfactant Solutions

Rouhollah Farajzadeh, Ali Barati, Harm A. Delil, Johannes Bruining, Pacelli L.J. Zitha¹



Delft University of Technology, Department of Geotechnology, Mijnbouwstraat 120, 2628 RX Delft, The Netherlands

¹ To whom correspondence should be addressed: Email: p.l.j.zitha@citg.tudelft.nl, Tel.: 31 (0)15 278 80437. Fax.: 31 (0)15 278 11 89R. Farajzadeh, SPE, H. Salimi, SPE, P.L.J. Zitha, SPE, and J. Bruining, SPE and Delft University of Technology

Copyright 2007, Delft University of Technology

This paper had been accepted for publication in Journal of Petroleum Science and Technology in January 2007.

Abstract

The mass-transfer of CO₂ into water and aqueous solutions of Sodium Dodecyl Sulphate (SDS) is experimentally studied using a PVT cell at different initial pressures and a constant temperature (T=25°C). It is observed that initially the transfer rate is much larger than expected from a diffusion process alone. The model equations describing the experiments are based on Fick's law and Henry's law. The experiments are interpreted in terms of two effective diffusion coefficients, one for the early-stages of the experiments and the other one for the later stages. The results show that at the early stages the effective diffusion coefficients are one order of magnitude larger than the molecular diffusivity of CO₂ in water. Nevertheless, in the later stages the extracted diffusion coefficients are close to literature values. It is asserted that at the early stages density driven natural convection enhances the mass transfer. A similar mass transfer enhancement was observed for the mass transfer between gaseous CO₂ rich phase with an oil (n-decane) phase. It is also found that at the experimental conditions studied addition of pure SDS does not have a significant effect on the mass transfer rate of CO₂ in water.

Keywords: *Mass Transfer, CO₂, Natural Convection, Effective Diffusion Coefficient, Surfactant*

1. Introduction

The mass transfer of a gas through a gas-liquid interface (with and without monolayers of surfactant) is of great importance in many fields of science and engineering. Examples include CO₂ sequestration, to reduce global heating effects (Holt et. al., 1994; Lindeberg and Wessel-Berg, 1997; Bachu and Adams, 2003; Yang and Gu, 2006), oil recovery (Zhang et. al, 2000; Nguyen et. al., 2002) and gas absorption (Vazquez et. al., 2000). There is a vast literature on the mass transfer between gas and liquids. We confine our interest to the experimental determination of the mass transfer rate of CO₂ into water in a PVT cell. It has been suggested in the literature that natural convection enhances the mass transfer (Lindeberg and Wessel-Berg, 1997; Yang and Gu, 2006).

Lindeberg and Wessel-Berg (1997) studied the conditions under which natural convection occurs as a result of CO₂ injection in saline aquifers. They found the following sequence of events: initially the injected CO₂ accumulates under the cap rock. Then, CO₂ dissolves into the reservoir brine by molecular diffusion. As a result, the density of brine increases, and therefore, natural convection occurs. Nevertheless, Lindeberg and Wessel-Berg (1997) did not quantify the effects of the natural convection in terms of enhanced mass transfer of CO₂ into the reservoir brine.

Yang and Gu (2006) studied the mass transfer of CO₂ into water at high pressures and temperatures. They interpreted the experimental results in terms of a modified diffusion equation and found an effective diffusion coefficient for each experiment. The effective diffusion coefficients were two orders of magnitude larger than the molecular diffusion coefficient. However the duration of their experiments were short (3-4 hours) and they did not study the long time behavior of the CO₂ mass transfer into water.

When surfactants are added to a quiescent liquid the total resistance to the transfer of gas molecules is the sum of the liquid phase resistance, the gas resistance and the interfacial resistance which arises from the adsorption of surfactant molecules to the interface. It has been shown that the presence of soluble surfactants has no measurable effect on the passage of gas molecules through the gas-liquid interface (Springer and Pigford, 1979; Caskey and Barlage, 1972; Hanwright et. al., 2005); however, insoluble surfactants can offer resistance to mass transfer (Koide and Orito, 1974; La Mer et. al., 1963; Blank, 1962; Barnes and Hunter, 1987; Barnes, 1997). To our knowledge the reported experiments in this area are conducted under atmospheric pressure and the effect of surfactants on mass

transfer at higher pressures apparently has not been reported in the literature.

In this report we study the mass transfer of CO₂ into bulk water and surfactant solutions experimentally to avoid the complex adsorption mechanism between surfactants and the porous medium. The emphasis of the paper is on the experimental results and procedure. In order to quantify the results we interpret the results in terms of two effective diffusion coefficients using a modified diffusion equation and leave a more complicated interpretation including natural convection for future work. This paper adds three contributions to the experimental knowledge base: Firstly, by extending the duration of the experiments we investigate the long term behavior of CO₂ mass transfer and investigate whether enhanced transfer persists over time or whether it dies out. Secondly, we perform the experiments with oil phase (in this paper n-decane) and show experimentally the enhancement of CO₂ mass transfer to the oil phase. Thirdly, this paper reports the effect of surfactants at high pressures. In section 2 we describe the experimental setup, materials and experimental procedure. In section 3 we define a model to interpret the experiments and in section 4 the obtained experimental data are incorporated into a physical model. This allows us to obtain two diffusion coefficients for the mass transfer process of CO₂ through a air-liquid interface; one for the early stages of the experiments and one for the late stages of the experiments. The possible mechanisms for the observed phenomena are discussed in section 5. We end our paper with some remarks and conclusions.

2. Experiments

2.1. Experimental setup

The experimental apparatus is shown in Fig. 1. It consists of a transparent scaled glass tube with an inner diameter of 7.0 mm, an outer diameter of 11.0 mm and a length of 45.0 cm. The tube was embedded in Teflon at the top and bottom and was sealed with o-rings and fitted inside a stainless steel cylinder. The glass tube has the capability of withstanding pressures up to 50 bar. To assure that the liquid is stagnant the stainless steel cylinder was mounted into a heavy (10 kg) steel holder. The bottom of the cell was equipped with a valve and a piston pump, which permitted injection of liquid into the cell. The top of the cell was connected to a high pressure gas cylinder. The gas pressure was measured with a calibrated pressure transducer with an accuracy of 5 mbar. Moreover, a safety valve was placed at the top part of the setup. A calibrated data acquisition system was provided to record the pressure and temperature in the cell during the experiment. The experimental data were recorded every 10 seconds by the computer. To avoid thermal fluctuations

the cell was located inside a liquid bath. In all experiments the bath was kept at 25±0.1°C.

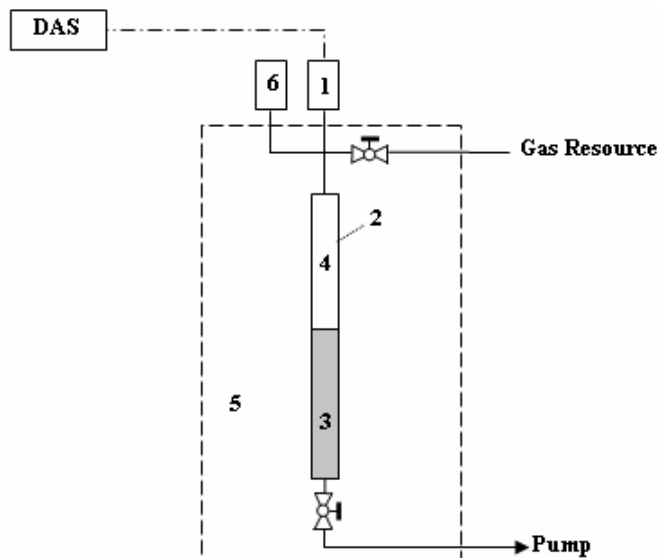


Figure 1: Schematic of the setup: The setup consists of a long tube in which the liquid phase and gas phase are brought in contact with each other at a certain pressure. The setup is held in a liquid bath with a constant temperature. The pressure of the gas in top part is monitored by a pressure transducer.

2.2. Materials and methods

Gas: The gas used to carry out the experiments was 99.98% pure carbon dioxide. CO₂ is highly soluble in water (Fogg and Gerrard, 1991), i.e., the Henry constant is 2980.1 Pa/mol/m³ (Sander, 1997). The diffusion coefficient of CO₂ in water is (1.97±0.10)×10⁻⁹ m²/s (Gertz et al., 1954). Nitrogen (N₂) was used to detect possible leakages in the setup.

Surfactant: The surfactant used to perform the experiments was Sodium Dodecyl Sulfate (SDS) with the chemical formula of C₁₂H₂₅SO₄Na and a molecular weight of 288 g/mol. It was dissolved in distilled water (pH = 5.5±0.1).

Before starting the experiments the Critical Micelle Concentration (CMC) of the surfactant was measured. To that end, solutions of SDS and distilled water with the concentrations of 2, 2.5, 3, 3.5, 4, 5 and 6 mmol/l were prepared. The surface tension of these solutions was measured by the DuNouy Ring method at room temperature. The apparatus was first calibrated with distilled water (the surface tension of distilled water at the

room temperature is 72.6 mN/m). The critical micelle concentration of the SDS was measured to be 0.6 mM at our experimental conditions.

2.3. Experimental procedure

In the pressure depletion experiments, the liquid phase was either pure distilled water or surfactant solutions with different surfactant concentrations. The concentration of the surfactant in some experiments was above the CMC and in some experiments below the CMC. For this purpose an appropriate amount of SDS was weighed and dissolved in distilled water. Originally some foam is formed at the surface, which collapses after leaving it undisturbed for a few minutes.

Before performing the experiments, the dry cell was filled with nitrogen to a certain pressure to assure that there is no leakage in the system. Fig. 2 shows the pressure versus time plot for a leakage test. The small fluctuations in the first part of the plot are due to small fluctuations in the temperature and the difference between the temperature of the gas cylinder and the liquid bath. The experimental procedure is as follows:

First, the liquid was injected from the bottom via an accurate piston pump into the cell until it reached the desired level. After that, pumping of the liquid was stopped and the valve at the bottom of the cell was closed. Next CO₂ was slowly injected into the cell from the top, for about 30 seconds. When the CO₂ pressure reached the desired value, the valve was closed and the cell was isolated. This was the starting time of the experiment. Each experiment was run for several days. All the experiments were repeated to show the reproducibility.

3. Physical model

3.1. Formulation

A physical model has been developed to describe the mass transfer based on Fick's law taking into account the solubility of the gas by Henry's law. The geometry of the problem under scrutiny is depicted in Fig. 3. The vessel consists of an upper column filled with gas and a lower column filled with a stagnant liquid layer. The model disregards convection and capillary effects. Moreover, it is assumed that the density of CO₂ in the gas phase only depends on time. We disregard both water evaporation (the contribution of water vapor to the gas pressure is 0.03 bar at 25°C (Greenwood and Earnshaw, 1997)) and water swelling due to CO₂ dissolution. Consequently we assume that the boundary remains fixed. The CO₂ concentration at the liquid surface is related to the gas pressure by assuming instantaneous thermodynamic equilibrium at the interface. We assert that the transfer of gas molecules through the gas-liquid interface can be described as a one dimensional unsteady-state diffusion process, i.e., by Fick's law. We take z positive in the downward direction

($z=0$ at the gas-liquid interface) and assume that diffusion coefficient does not change significantly with concentration. Since the liquid column is large the concentration is taken zero at the bottom of the vessel. The gas inside the vessel follows the real gas law and the gas pressure can be calculated by $PV = ZRT$.

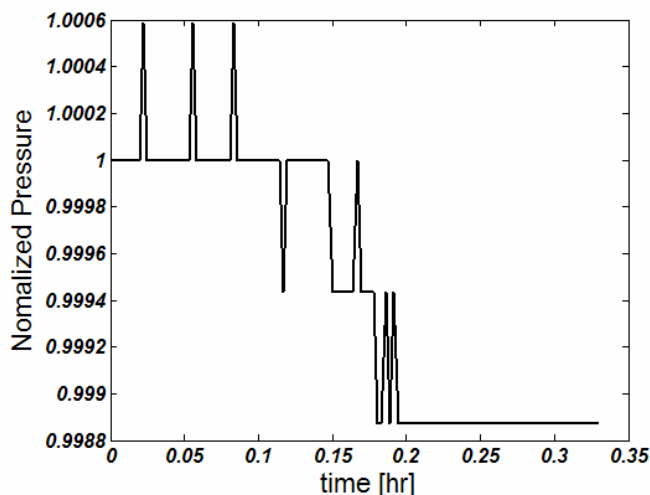


Figure 2: Leakage test: The setup was checked for any possible leakage by injecting nitrogen. The pressure should be constant with time in the range of accuracy of the pressure transducer.

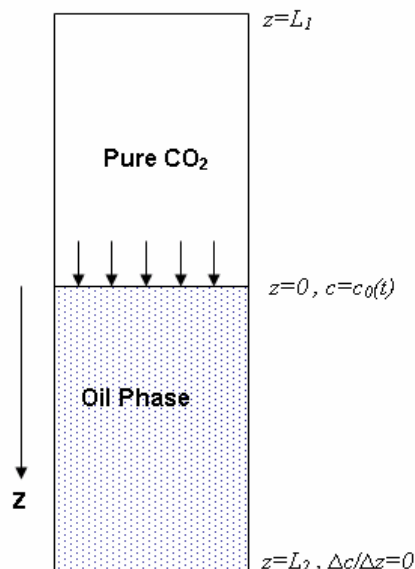


Figure 3: Schematic outlay of the process: The total length of the tube is L , the height of water is L_2 and the height of the gas is L_1 . There is no gas flowing out at the end of the tube. The gas-liquid interface is fixed. The liquid concentration at the interface is related to the gas pressure through Henry's law and changes with time.

3.2. Equations

For this system Fick's second law can be written as

$$\frac{\partial c}{\partial t} = D \frac{\partial^2 c}{\partial z^2} \quad 0 \leq z \leq L_2, 0 \leq t \leq \infty \quad (1)$$

where, D is the effective diffusion coefficient and c is the concentration of CO_2 in the liquid phase. Initially there is no gas inside the liquid, i.e.

$$c(z, t=0) = c_0 = 0. \quad (2)$$

Since the diffusion process is slow and the liquid column is large, we can assume that the concentration of the gas is zero at the end of the tube ($L_2 \rightarrow \infty$). The second boundary condition is given by Henry's law which states that the pressure of a gas above a solution is proportional to the mole fraction (concentration) of the gas in the solution, i.e.,

$$P(t) = Hc(t), \quad (3)$$

where H is taken as Henry's law proportionality constant. An additional condition to the present problem can be written in accordance with the fact that the change of the total moles of gas in the system is due to diffusion into the liquid. The mass flux of the gas at the interface for real gas can be written as

$$\left. \frac{dn_g}{dt} \right|_{z=0} = \frac{V}{ZRT} \left. \frac{dP_g}{dt} \right|_{z=0} = -DS \left. \frac{\partial c}{\partial z} \right|_{z=0}, \quad (4)$$

where V and S are the gas volume and the cross-sectional area of the cell respectively, R is the universal gas constant and Z is the compressibility factor. V is also assumed to be constant (no moving boundary).

By substituting Henry's law for the gas pressure in Eq. (4) we obtain

$$-DS \left. \frac{\partial c}{\partial z} \right|_{z=0} = \frac{VH}{ZRT} \left. \frac{\partial c}{\partial t} \right|_{z=0}. \quad (5)$$

3.3. Analytical solution

Eq. (1) has a time dependent boundary condition and can be solved by Laplace transform method. Laplace form of Eq. (1) is

$$\frac{\partial^2 \bar{C}}{\partial z^2} - \frac{s}{D} \bar{C} = 0. \quad (6)$$

The final solution of Eq. (6) with the given boundary conditions is

$$\bar{C}(s) = \frac{1}{\frac{H}{P_i} s - \frac{ZRT\sqrt{D}}{L_1 P_i} \sqrt{s}} \exp\left(-\sqrt{\frac{s}{D}} z\right). \quad (7)$$

Applying Laplace transform to Eq. (4) and using Eq. (7) yields

$$\frac{L_1}{ZRT} (s\bar{P}_g - P_i) = -\frac{1}{\frac{H}{P_i \sqrt{D}} \sqrt{s} - \frac{ZRT}{P_i L_1}}, \quad (8)$$

from which we can obtain

$$\frac{\bar{P}_g(s)}{P_i} = \frac{1}{s} - \frac{1}{\frac{L_1 H}{ZRT\sqrt{D}} s^{3/2} - s}. \quad (9)$$

The gas pressure as a function of time is found by Laplace inversion as

$$P_g(t) = P_i \left[2 - \exp(\kappa^2 t) \operatorname{erfc}(-\kappa\sqrt{t}) \right], \quad (10)$$

where

$$\kappa = \frac{ZRT\sqrt{D}}{L_1 H}. \quad (11)$$

Due to our boundary condition –that the concentration is zero at the bottom of the cell ($z = L_2$) we find as long time behavior that the pressure is declining indefinitely. However, that occurs for times much longer than relevant for the experiment.

It should be also mentioned that the solution of Fick's second law assuming a constant concentration at the gas-liquid interface suggests that after a long time the concentration at the interface is linearly proportional to the square root of time, i.e., the plot of gas pressure versus the square root of time will be a straight line (Coulson and Richardson, 1977).

4. Results and Discussion

4.1. Pressure decline

In this study, the quantification of the mass transfer rate is based on the measurement of the gas pressure in a closed volume containing a column of liquid below a gas column. The changes in the gas pressure are assumed to be only due to transfer of gas into the liquid phase. The measured gas pressure versus time for both distilled water and the surfactant solution are plotted for all experiments. The general trends of the curves for different initial pressures were similar. Thus due to these similarities only the curves of Exp2 will be presented in this paper.

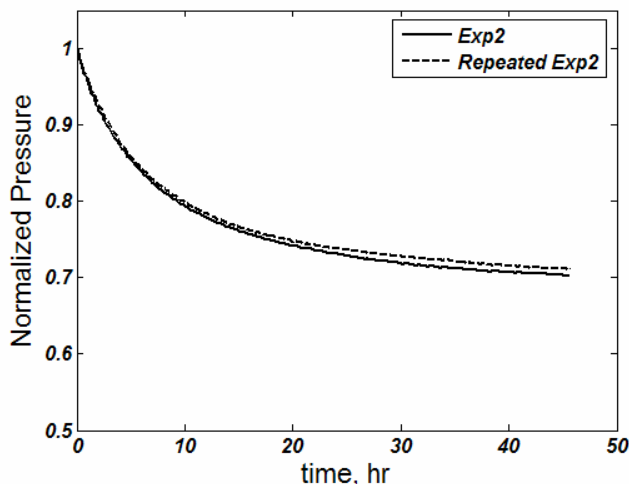


Figure 4: Reproducibility test: All of the experiments were repeated to assure that the observed pressure decline is only due to the mass transfer of CO₂ into water and the obtained data are reproducible.

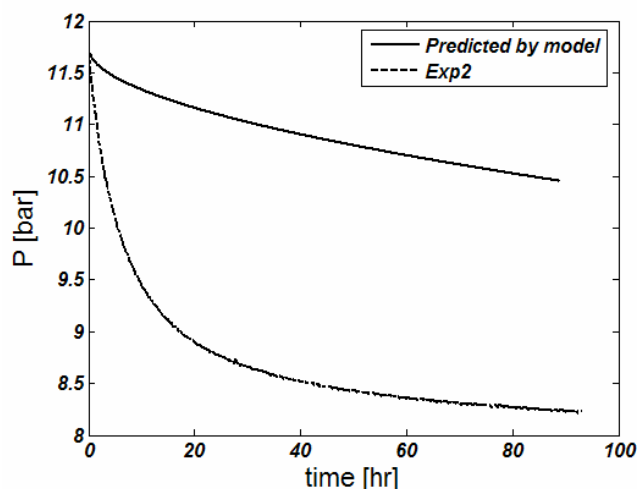


Figure 5: Comparison between experiment and model: This curve shows the comparison between the model which is based on the modified Fick's second law and the experimental data. At the initial stages of the experiments the rate of mass transfer of CO₂ into water is higher than the predicted values by the physical model.

However, the extracted data will be reported for all experiments (Table 1-2).

Fig. 4 shows normalized CO₂ pressure versus time during pressure decline measurements for Exp2. It shows that the gas pressure decreases with time due to the transfer of the CO₂ molecules into water. Comparison between the solid and dashed lines in the figure shows the reproducibility of the experiment. The small difference between these two curves is due to the difficulties in setting the initial pressure to the same value for the two experiments

It becomes clear from Fig. 4 that the gas pressure declines significantly at the initial stages of the experiment, i.e., has a steep slope at the early times of the experiment. However, the slope of the curve becomes less steep with time, meaning that also the mass transfer rate decreases with time. Fig. 5 shows the comparison between the measured pressures and the model using the known diffusion coefficient of CO₂ in water (in this curve chosen to be $D=1.97 \times 10^{-9} \text{ m}^2/\text{s}$). The curve shows significant discrepancy between experimental and predicted values.

4.2. Deviation from the square root of time

Fig. 6 shows the plot of the measured gas pressure versus the square root of time for Exp2. It shows that the initial behavior of this curve is faster than the square root of time. This is an indication of the higher mass transfer of CO₂ into water, which cannot be explained by a diffusion like process. Interestingly, after about one day the pressure vs. square root of time curve becomes linear. It can be expected that at longer times the mass transfer of CO₂ into water is determined by molecular diffusion.

4.3. Estimated diffusion coefficients

In this paper two effective diffusion coefficients are extracted from the experimental data describing the initial and long-time behavior of the CO₂ mass transfer into water and surfactant solutions. The procedure is as follows:

In the plots of pressure versus square root of time (for example Fig. 6 for Exp2), the late-stage experimental data are fitted to a straight line. The intercept of the fitted line in Fig. 6 is the initial pressure with which the mass transfer process would have started if diffusion had been the only responsible mechanism for mass transfer of CO₂ into the liquid (no convection case). Therefore, to obtain the late-stage diffusion coefficient this pressure is put as initial pressure in the physical model, for which the model equation is Fick's second law with a time dependent boundary condition. The lower solid curve in Fig. 7 is the predicted gas pressure by Eq. (10) using the initial pressure obtained from Fig. 6 and choosing $D = 2.75 \times 10^{-9} \text{ m}^2/\text{s}$ and inserting the literature value of Henry's coefficient ($H = 2980.1 \text{ Pa}/\text{mole}/\text{m}^3$). The dashed line shows the experimentally measured pressure data versus time. With a diffusion coefficient close to the molecular diffusion coefficient of CO₂ into the water the predicted values by the model are in excellent agreement with the measured pressure values. To obtain the effective coefficients for early stages of the experiments the experimental initial pressure was put in the model and the effective diffusion coefficient was obtained with the help of the data. The upper solid curve in Fig. 7 is the predicted gas pressure by Eq. (10) choosing $D = 8.35 \times 10^{-8} \text{ m}^2/\text{s}$ and $H = 2980.1 \text{ Pa}/\text{mole}/\text{m}^3$. Alternatively we can use

the later stage diffusion coefficient $D = 2.75 \times 10^{-9} \text{ m}^2/\text{s}$ but then the Henry's coefficient needs to be modified to $H = 552.01 \text{ Pa/mole/m}^3$. Such a small value has not been reported in the literature for CO_2 solubility in water. Therefore, we have chosen to use the literature value of Henry's coefficient in the interpretation of the experiments.

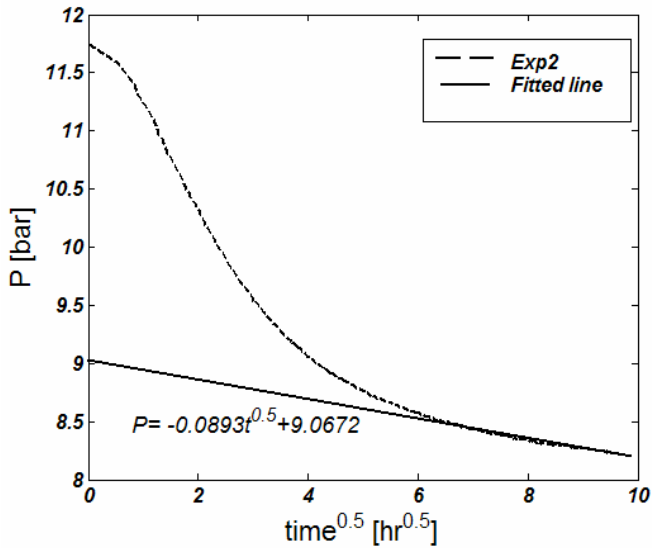


Figure 6: Measured pressure data plotted versus the square root of time. The long time part of the experiment can be fitted to a straight line.

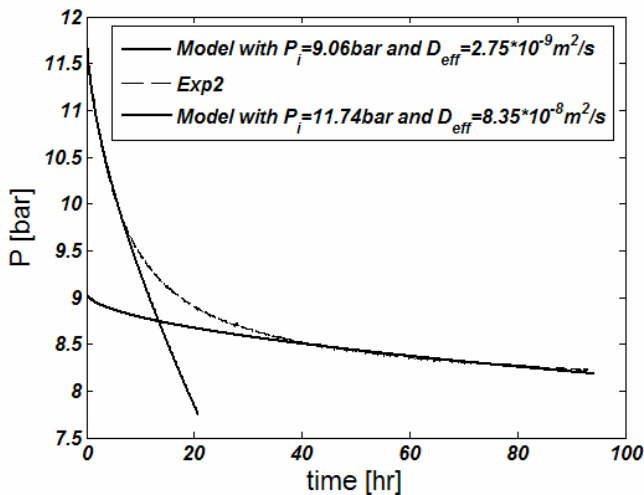


Figure 7: Extraction of diffusion coefficients, using Eq. (10): the data are fitted to two curves of the form suggested by Eq. (10). The lower solid line shows the predicted pressure values using the virtual initial pressure obtained from Fig. 8 and $D = 2.75 \times 10^{-9} \text{ m}^2/\text{s}$. The dashed line is the measured pressure data. The left solid line shows the predicted pressure values using the real pressure obtained from Fig. 8 and $D = 8.35 \times 10^{-8} \text{ m}^2/\text{s}$.

The extracted effective diffusion coefficients for different experiments are shown in Table 3. The obtained effective diffusion coefficients for the early stages of the experiments are one order of magnitude larger than the actual molecular diffusion of CO_2 into water, again indicating the faster mass transfer rate of CO_2 into water at the early stages of the experiment. However, the obtained effective diffusion coefficients for the later stages of the experiments imply that after a certain time, the mass transfer of CO_2 into aqueous solutions becomes slower compared to the initial stages. The early-stage diffusion coefficients increase with increasing initial pressure proving the fact that even at slightly high pressures for CO_2 -water system the diffusion coefficient is a strong function of the initial pressure, i.e., the initial concentration of CO_2 in the system. This means that at higher pressures the effective diffusion coefficients will be even higher. This observation is also supported by the experimental results in Yang and Gu (2006) in which the authors found diffusion coefficients which were two orders of magnitude larger than the molecular diffusion coefficient of CO_2 into water at higher pressures. In addition, that regardless of the initial pressure, after a certain time, diffusion becomes the dominant mechanism for mass transfer of CO_2 into water. The diffusion coefficient extracted from the long time behavior turns out to be independent of the initial experimental pressure.

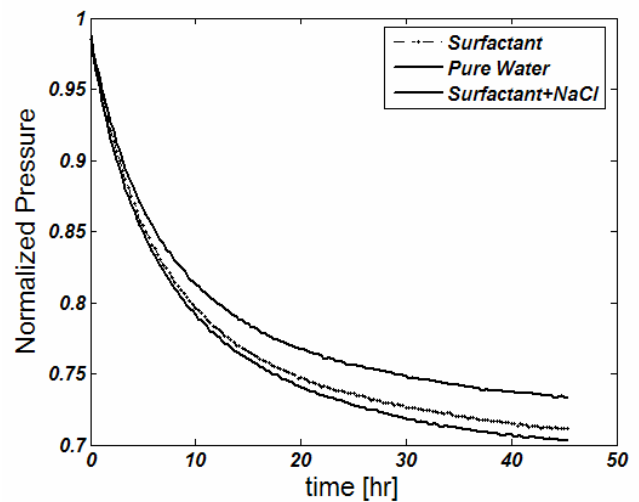


Figure 8: Comparison of measured pressure data for pure water, solution of water and SDS and solution of water and surfactant with NaCl versus time.

4.4. Influence of surfactant

To study the influence of the soluble surfactants on the interfacial mass transfer some of the experiments were done using surfactant solutions of SDS as liquid phase. Fig. 8 shows the normalized pressure decline curve for the experiments with surfactant solution together with the

experiment with pure water. It is evident from Fig. 8 that at our experimental conditions the addition of soluble surfactant (SDS) has no significant effect on mass transfer rate of CO₂ into water. However, it seems that addition of salt slightly retards the mass transfer. Several parameters can be responsible for this behavior: (a) the addition of NaCl increases the viscosity of the solution and therefore the effective diffusion coefficient decrease by adding NaCl, (b) the addition of NaCl decreases the solubility of CO₂ in water. Therefore, less CO₂ is dissolved in water in the experiment with NaCl compared to experiments without NaCl and (c) the addition of salt increases the adsorption of the surfactant molecules at the interface (Santanu and Pak, 2006) and the interface becomes more packed which could be another possible reason for the differences of the curves in Fig. 8. Our results are consistent with the results of other researchers (La Mer et al., 1963; Molder et al., 1998; Raymond and Zieminski, 1971), i.e., the surface resistance for soluble surfactants is very small. However, the insoluble surfactants do have a significant effect on the transfer rates of gas through the gas-liquid interface.

The same procedure as discussed above was also followed to extract the effective diffusion coefficients for surfactant solutions. Indeed, the obtained diffusion coefficient values for surfactant solutions are about the same as for the experiments with water and are presented in Table 3.

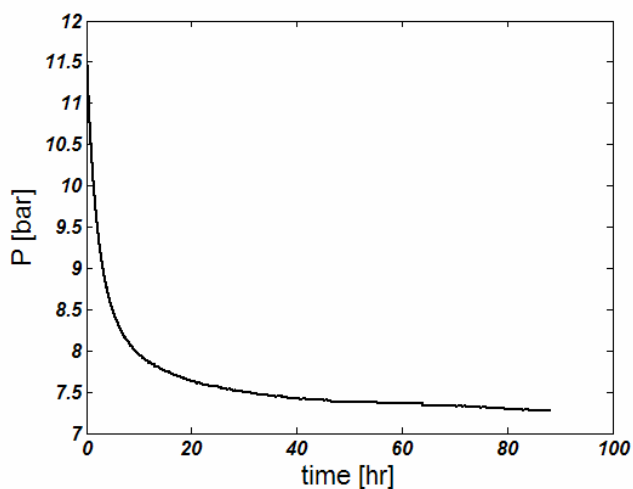


Figure 9: Pressure decline curve in the experiment with n-decane. The pressure behavior is similar to the water case, indicating an enhancement of mass transfer in the initial stages of the experiment. In long time the conventional diffusion behavior is observed.

4.5. Experiment with n-decane

We carried out a few experiments to study the mass transfer of CO₂ into hydrocarbons from which we report the obtained pressure curve from a experiment with n-decane. The dissolution of CO₂ increases the density of the

hydrocarbons (Ashcroft and Ben Isa, 1997). The experimental procedure and conditions were the same as explained in section 2. The initial pressure of the experiment was 11.85 bar. Fig. 9 shows that initially the mass transfer of CO₂ is faster than at the later stages. We believe that this result has implications for enhanced oil recovery for CO₂ flooding and improved oil recovery in fractured oil reservoirs.

5. Possible mechanisms

As an explanation for the observed discrepancy between the physical model and the experimental data in Fig. 5 the following possibilities have been considered.

a) CO₂ may be adsorbed to the water “attached” to the gas filled part of the glass tube. This explanation is however unlikely because it requires a water layer thickness of 2mm.

b) Other possibilities are related to the validity of Henry’s law in relating the surface concentration of the fluid to the gas pressure. Even if we consider these possibilities less likely, they have to be investigated.

c) When CO₂ is brought into contact with water, the dissolution and diffusion of CO₂ leads to a concentration gradient in the water and also a density gradient (Gmelin, 1973). As the density increases with increasing dissolution of CO₂ at the interface, the fluid on top of the water near the interface becomes denser. This density gradient induces natural convection to the system which speeds up the transfer of CO₂ into water and results in higher flux of CO₂ at the interface. However, the density gradient and therefore natural convection effects, decreases with time and after a certain time the density gradient is not large enough to sustain convection to the system.

In addition to the natural convection, the time-dependency of the boundary condition in Eq. (4) can be another reason why the early pressure history is not proportional to the square root of time. However, as we can see from Fig. 6 the pressure decline is slow at the later stages and then the gas pressure can be considered constant for the boundary condition.

The observations mentioned above can be quantified in terms of the effective diffusion coefficients. It is seen that regardless of the initial pressure, after a certain time, the enhancement effects will be less and diffusion becomes the dominant mechanism for CO₂ mass transfer CO₂ into water.

Furthermore, as can be seen from Fig. 9 it appears that natural convection is also responsible for the mass transfer of CO₂ into n-decane (oil phase). Once more, at the later stages the effect of natural convection becomes less significant.

6. Conclusions

- In this paper it is shown that a relatively simple PVT cell can be used to study the enhanced mass transfer between gases and liquids.
- A physical model based on the Fick's second law and Henry's law can be used to interpret the experimental data. We use the model to extract two diffusion coefficients.
- The mass transfer process cannot be modeled with a modified Fick's second law with a single effective diffusion coefficient.
- The initial stages and later stages of the experiments could be modeled individually with the described model and two effective diffusion coefficients could be obtained from the experimental data.
- The obtained effective diffusion coefficient values for the initial stages of the experiments were one order of magnitude larger than the molecular diffusivity. It was suggested that at the early stages of the experiments density-driven natural convection enhances the mass transfer of CO₂ into water.
- The effective diffusion coefficients for the initial stages of the experiments increase with increasing pressure.
- The extracted diffusion coefficients for the later stages of the experiments agree with the molecular diffusivity of CO₂ into water. It was asserted that after a certain time, the density driven natural convection becomes less important. At the later stages diffusion becomes the dominant mechanism for the mass transfer experiments of CO₂ into water and surfactant solutions.
- The same behavior was seen from the surfactant solution experiments. Moreover, the results of experiments show that the addition of SDS to water has no measurable effect on the mass transfer rate in our experimental setup.
- A similar mass transfer enhancement was observed for the mass transfer between gaseous CO₂ rich phase with an oil (n-decane) phase. This has implications for the oil recovery.

7. Acknowledgments

This work was funded by a special program of the TU Delft, Delft Earth Research. We thank the staff of Dietz laboratory of our faculty, especially H. van der Meulen and P. de Vreede for their technical support.

8. Nomenclature

c = Gas concentration [M]

\bar{C} = Laplace transform of c [M]

D_{eff} = Effective diffusion coefficient [m²/s]

H = Henry's constant [Pa/ mol/m³]

L = Length of the experimental tube [m]

L_1 = Height of the gas in the experimental tube [m]

L_2 = Height of the liquid in the experimental tube [m]

P_g = Gas pressure [Pa]

P_i = Initial gas pressure [Pa]

R = Universal gas constant [J/mol/K]

S = Cross sectional area of the tube [m²]

t = time [sec]

T = Temperature [K]

V = Volume of the gas in tube [m³]

Z = Gas compressibility factor [-]

9. References

1. Ashcroft S. and Ben Isa M., Effect of dissolved gases on the densities of hydrocarbons, J. Chem. Eng. Data, 1997, 1244-1248.
2. Bachu S., Adams J.J., Sequestration of CO₂ in geological media in response to climate change: capacity of deep saline aquifers to sequester CO₂ in solution, Energy Convers. Manage., 2003, 44, 3151-3175
3. Barnes G.T., Hunter D.S., The evaporation resistance of monolayers of cellulose decanoate, J. Colloid Interface Sci., 1989, 129, 585-587
4. Barnes G.T., Permeation through monolayers, Colloids Surf. A, 1997, 126, 149-158
5. Blank M.J., Monolayer Permeability and the Properties of Natural Membranes, Phys. Chem., 1962, 66, 1911-1918
6. Caskey, J.A., Barlage W.B. Jr., A study of the effects of soluble surfactants on gas absorption using liquid laminar jets, J. Colloid Interface Sci., 1972, 41, 52-62.
7. Coulson J.M., Richardson J.F., Chemical Engineering, 3rd ed., Pergamon Press, Oxford, 1977, Vol. 1, pp 281-286.
8. Fogg P.G.T., Gerrard W., Solubility of gases in liquids, Wiley, New York, 1991, pp 281-314.

9. Gertz Kh., Loeschcke Hh., *Helv. Physiol. Pharmacol. Acta.*, 1954, 12(4) : C 72-4.
10. Gmelin L., *Gmelin Handbuch der anorganischen Chemie*, 8. Auflage. Kohlenstoff, Teil C3, Verbindungen., 1973, pp 64-75.
11. Greenwood N.N. and Earnshaw A., *Chemistry of the elements*, 2nd Ed. Butterworth Heinemann, Oxford, 1997.
12. Hanwight J., Zhou J., Evans G.M., Galvin K.P., *Influence of Surfactant on Gas Bubble Stability*, *Langmuir*, 2005, 21, 4912-4920
13. Holt T., Jensen J., Leindeberg E., *Underground storage of CO₂ in aquifers and oil reservoirs*, *Energy Convers. Manage.*, 1994, 36, 535-538
14. Koide K., Orito Y. and Hara Y., *Mass transfer from single bubbles in Newtonian liquids*, *Chem Engng Sci.* 1974, 29, 417
15. La Mer V.K., Aylmore L.A.G., Healy T.W., *The ideal surface behavior of mixed monolayers of long chain n-paraffinic alcohols*, *J. Phys. Chem.*, 1963, 67, 2793-2795
16. Lindeberg E., Wessel-Berg D., *Vertical convection in an aquifer column under a gas cap of CO₂*, *Energy Convers. Manage.*, 1997, 38, S229-S234
17. Molder E., Tenno T., Nigu P., *The Influence of Surfactants on Oxygen Mass Transfer through Air-Water Interface*, *Critical Rev. Anal. Chem.*, 1998, 28, 75-80
18. Nguyen P., Zitha P.L.J., Currie P.K., *Effect of foam films on gas diffusion*, *J. Colloid and Int. Sci.*, 2002, 248, 467-476
19. Raymond D.R. and Zieminski S. A., *Mass transfer and drag coefficients of bubbles rising in dilute aqueous solutions*, *A.I.Ch.E.J.*, 1971, 17, 57
20. Sander R, *Compilation of Henry's Law Constants for Inorganic and Organic Species of Potential Importance in Environmental Chemistry*, <http://www.mpch-mainz.mpg.de/%7Esander/res/henry.html>, Version 3, 1999, p57
21. Santanu Paria and Pak K. Yuet, *Effects of Chain Length and Electrolyte on the Adsorption of n-Alkylpyridinium Bromide Surfactants at Sand-Water Interfaces*, *Ind. Eng. Chem. Res.*, 2006, 45, 712-718.
22. Springer T.G., Pigford R.L., *Influence of Surface Turbulence and Surfactants on Gas Transport through Liquid Interfaces*, *Ind. Eng. Chem. Fundam.*, 1970, 9, 458-465.
23. Vazquez G., Antorrena G., Navaza J.M., *Influence of Surfactant Concentration and Chain Length on the Absorption of CO₂ by Aqueous Surfactant Solutions in the Presence and Absence of Induced Marangoni Effect*, *Ind. Eng. Chem. Res.*, 2000, 39, 1088-1095
24. Yang Ch., Gu Y., *Accelerated mass transfer of CO₂ in reservoir brine due to density-driven natural convection at high pressures and elevated temperatures*, *Ind. Eng. Chem. Res.*, 2006, 45, 2430-2436
25. Zhang Y.P., Hyndman C.L., Maini B.B., *Measurement of gas diffusivity in heavy oils*, *J. Petroleum Sci. and Eng.*, 2000, 25, 37-47

Table 1: List of Experiments with water

Experiment Number	Initial Pressure (bar)	Temperature (°C)
Exp1	7.72	25±0.1
Exp2	11.73	25±0.1
Exp3	20.10	25±0.1

Table 2: List of Experiments with SDS solution

Experiment Number	Initial Pressure (bar)	T (°C)	SDS Concentration
Exp4	11.80	25±0.1	C=30mM>CMC
Exp5	11.76	25±0.1	C < CMC
Exp6	11.75	25±0.1	C=30mM+NaCl

Table 3: The late-stage and early stage effective diffusion coefficients extracted from experimental data. The effective diffusion coefficients in the third and fourth columns were extracted by choosing the literature value of Henry's coefficient, $H= 2980.1 \text{ Pa/mol/m}^3$

Experiment Number	\sqrt{D} / H	D_{eff} for early stages (m^2/s)	D_{eff} for later stages (m^2/s)
Exp1	7.00×10^{-8}	4.35×10^{-8}	2.05×10^{-9}
Exp2	9.50×10^{-8}	8.35×10^{-8}	2.75×10^{-9}
Exp3	1.10×10^{-7}	10.70×10^{-8}	2.05×10^{-9}
Exp4	9.46×10^{-8}	7.95×10^{-8}	2.50×10^{-9}
Exp5	9.37×10^{-8}	7.80×10^{-8}	3.50×10^{-9}
Exp6	9.00×10^{-8}	7.20×10^{-8}	1.95×10^{-9}